

Design of a Flat Membrane Module for Fouling and Permselectivity Studies

A. Santafé-Moros* and J.M. Gozávez-Zafrilla

Institute for Industrial, Radiological and Environmental Safety (ISIRYM), Universidad Politécnica de Valencia, Spain

*Universidad Politécnica de Valencia (Dpto. Ing. Química y Nuclear, Ed. 5L). C/ Camino de Vera s/n. 46022 Valencia. Spain, E-mail: assanmo@iqn.upv.es

Abstract: Flat membrane modules of laboratory scale are commonly used to study membrane performance. As membrane performance is influenced by pressure and velocity, it is important to have hydrodynamics conditions as uniform as possible over the membrane surface. However, most modules designed for laboratory studies have high pressure drop and abrupt changes of flow direction what yields to lack of uniform flow and uncertainty of the pressure value over the membrane surface.

In this paper, we explain how COMSOL was used to design a module intended to minimize these drawbacks. The Incompressible Navier-Stokes mode was used to optimize the geometry of the fluid chamber while the solid stress-strain mode was used to improve the mechanical performance of the module. Fluid dynamic computation results were evaluated with experimental results obtained with the module prototype.

Keywords: Membrane, Module, Fouling, permeation.

1. Introduction

Flat membrane modules of laboratory scale are commonly used to study membrane performance. The research with this type of module is a previous phase to the use of commercial spiral-wound modules of much greater area because they have the following advantages:

- The operating conditions can be controlled more effectively in a small scale module.
- The results observed can be related with specific properties of the membrane element and are not masked by lack of membrane uniformity.
- The small membrane area required makes the experimentation more economical, especially when destructive tests are performed.

In a pressure-driven membrane process, a pressurized feed enters in the module where the membrane is placed (Figure 1). Thanks to the difference of pressure existing between both membrane sides a permeation flow through the membrane occurs. As the membrane is a permselective barrier, a stream more concentrated in the components rejected by the membrane is produced (retentate stream). A common experimental set-up for membrane characterization is shown in Figure 2. Note that typically two manometers are placed in the feed and retentate ducts in order to have an estimation of the average pressure inside the module.

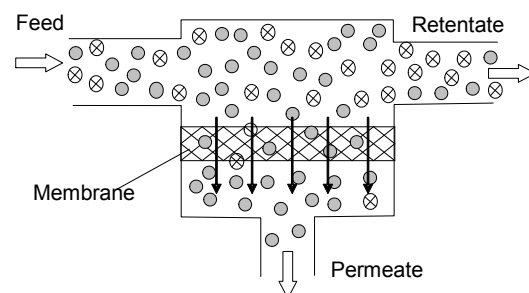


Figure 1. Scheme of a flat membrane module.

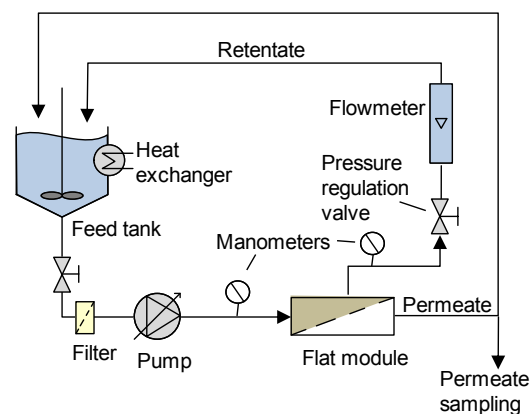


Figure 2. Typical experimental set-up incorporating a flat membrane module.

In the case of pressure-driven processes, the relevant operating conditions to membrane performance are pressure, velocity, temperature and feed characteristics (i.e. composition, concentration and pH) [1]. A thorough control and measurement of these variables is needed to obtain useful information. The temperature can be maintained constant by means of a thermostat. Feed characteristics can be maintained constant if permeate and retentate are continuously recycled back to the feed tank. Pressure and feed flow can be established by using a volumetric speed-variable pump and a regulation valve placed in the retentate duct. Pressure is the main driving-force for permeate flow. Feed flow determines the cross-flow velocity on the membrane surface which reduces the concentration polarization on the boundary layer next to the membrane surface. Concentration polarization has influence on membrane rejection and fouling of the membrane surface [2].

Therefore, in order to accurately relate pressure and cross-flow velocity with membrane performance is necessary to have hydrodynamic conditions as uniform as possible over the membrane surface. However, many modules designed for laboratory use have high pressure drop and abrupt changes of flow direction what yield to lack of uniform flow and uncertainty of the true pressure value along the membrane surface.

The use of CFD techniques is an efficient tool to improve commercial and laboratory modules. Different research groups have studied the effects of flow on concentration polarization [3-11] or the membrane transport and fouling [12-23]. In particular, in collaboration with other research group, we used COMSOL to study the effects of flow distribution on fouling for a laboratory module [24].

In this work, we have used COMSOL Multiphysics in the design phase of a new laboratory module intended to have more uniform flow profile and make possible accurate pressure measurement. The main characteristic of this module is the presence of two chambers connected to the membrane chamber through a groove along the width of the membrane chamber (Figure 4). One is placed immediately after the module input, the other one before the output. These chambers have a double functionality: homogenization of the flow profile and accurate measurement of pressure as the

manometers are directly connected to the chambers.

The rest of the paper is divided into the following parts: First, we explain how COMSOL was used to perform the fluid dynamic study of the module. Second, we show the mechanical modeling to verify that the model is able to resist an operating pressure of 60 bar (6 MPa). Third, the effect of input position and the position of the stabilizing chambers is discussed. Fourth, the mechanical performance of the design obtained is assessed. Finally, the conclusions of the work are shown.

2. Fluid dynamic modeling of the module

2.1 Domain geometries

Conventional flat module geometry has typically a plate-and-frame structure like that illustrated in Figure 3. The membrane is placed between two plates that are press together. The feed stream enters to a distribution duct and descends through a groove to the membrane chamber. A U-shape or zigzag-shape flow is established in the chamber depending on where the collecting point of the retentate stream is placed. The membrane lies on a porous support that collects the permeate that has passed through the membrane towards the permeate collector.

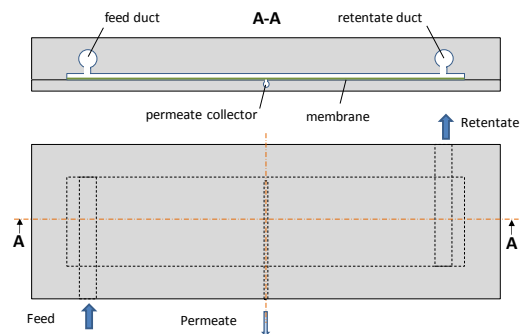


Figure 3. Geometry of conventional flat membrane module and module.

To avoid the inconvenience of flow asymmetry, we decided to build a module with two inputs and two outputs (Figure 4). The feed stream is previously split into two streams of the same flow so that two identical retentates and a symmetrical flow profiles are expected. Taking

into account the symmetry of the problem, the domain geometry was only half of that of the module (Figure 5). It was performed in 2D and then extruded to a 3D geometry. However, the studies intended to obtain an optimal position of the chambers for pressure stabilization were performed using a much simpler geometry in 2D (Figure 6).

The height of the membrane chamber was 1 mm. The preliminary results indicate the convenience of having chambers of 0.2 mm at the edges between the grooves and the membrane chamber.

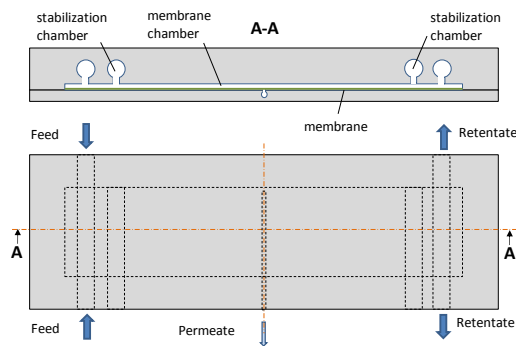


Figure 4. Geometry of the module with chambers for pressure measurement.

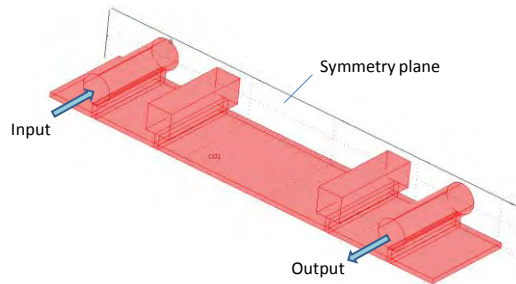


Figure 5. Simplified 3D geometry of the flow domain.

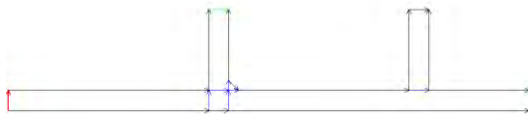


Figure 6. Simplified 2D geometry of the flow domain.

2.2 Governing equations

Typically, a laboratory module is used with a turbulent promoter (similar to a net) placed inside the membrane chamber. Then, a flatter profile of averaged velocity distributions is obtained and local turbulent conditions can be obtained. However, we thought in laminar conditions as a limiting case of less uniform velocity profile. Besides, sometimes there is a special interest in studying laminar conditions in a module, as the value of the shear rate over the membrane surface is clearly defined [24]. This analysis has interest in studies on fouling and concentration polarization effects.

Therefore, we used the Incompressible Navier-Stokes mode of Chemical Engineering toolbox in stationary mode which is based on the use of the stationary Navier-Stokes (1) and the continuity (2) equations.

$$\nabla \cdot \eta (\nabla \mathbf{u} + (\nabla \mathbf{u})^T) + \rho (\mathbf{u} \cdot \nabla) \mathbf{u} + \nabla p = 0 \quad (1)$$

$$\nabla \cdot \mathbf{u} = 0 \quad (2)$$

2.3 Boundary conditions

The liquid properties used were those of water at 20 °C ($\rho = 1000 \text{ kg} \cdot \text{m}^{-3}$, $\eta = 1.002 \times 10^{-3} \text{ Pa} \cdot \text{s}$).

For the 2D geometry the input boundary condition was set as a laminar input of average velocity of 1 m/s. For two parallel plates, the characteristic dimension is twice the distance between the plates and the value of Reynolds number corresponds to laminar conditions ($Re \cong 2000$). The boundary condition for the output was set at zero pressure condition. The non-slip wall condition was set in the rest of the boundaries.

For the 3D geometry the input boundary condition was set at the average velocity of 0.707 m/s that corresponded to an average velocity of 1 m/s in the membrane chamber. The output was initially set as a laminar outflow conditions and then turn up to a pressure zero condition in a posterior calculation. The symmetry boundary condition was used in the surfaces contained in the symmetry plane. The non-slip wall condition was set in the rest of the surfaces.

2.4 Meshing

The mesh for the 3D geometry of the fluid domain is shown in Figure 7. It was performed by extruding a 2D geometry meshed using a quad-mesh. As the flow chamber was very thin, a structured mesh was used in order to minimize the number of mesh elements.

The mesh for the simplified 2D geometry consisted of 11500 triangular elements.

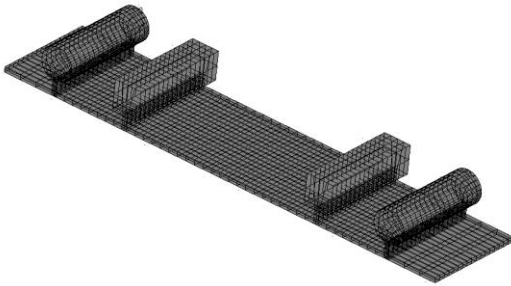


Figure 7. Mesh for the 3D fluid domain.

2.5 Solver used

The problem was solved in a single computer (Intel Core 2 Quad CPU 2.40 GHz).

The simplified 2D problem had 53000 DOF and could be solved using the direct solver PARDISO. The 3D problem had much higher number of DOF (152000), therefore, an iterative Linear System Solver (GMRES) was used. SSOR was selected as an efficient preconditioner for the problem.

3. Mechanical modeling of the module

The “Solid, Stress-Strain mode” was used to study the mechanical performance of the final design of the module. It was considered interesting to determine if the bolts used to press together the two module plates were correctly placed and if the holes drilled on the metal block did not excessively debilitate the piece. The module was conceived to work at pressures of 60 bar (6 MPa) but a security factor of 2 was applied in the calculations.

3.1 Domain geometry

In this case two domain geometries were modeled (the upper and the lower plates of the module with the fluid domain excluded) and separately calculated. As calculation was faster enough, we did not take advantage of the domain symmetry.

The two plates are fixed together with 10 bolts to support pressure. The upper plate has a thickness of 15 mm and the input and output ducts and the chambers for pressure measurement are drilled in it. The lower plate has a thickness of 10 mm and only the permeate channel is drilled in it.

3.2 Subdomains and boundary settings

The material properties were those of steel AISI properties taken from the COMSOL library material.

When there is pressure inside the membrane chamber, the bolts apply the force at the washers to maintain the two plates of the module together. Therefore, in the areas in contact with the washers the boundary condition was set as a z-displacement constraint ($R_z = 0$). In the faces in contact with the fluid, the boundary condition was a load with the value of the pressure normally applied to the surface.

3.3 Meshing and solver used

Triangular meshes were applied to each subdomain (10920 and 2830 mesh elements for the upper and lower plate respectively).

The direct solver SPOOLES was applied to solved the problem.

4. Fluid dynamic results

The space between the two chambers for pressure measurement is the useful area for membrane characterization. Therefore, the flow profile must be completely developed. The 2D simplified geometry was used to study where the flow profile stabilizes after the abrupt change of direction that suffers the flow entering from the distributor to the membrane chamber (Figure 8). This position was selected to place the chambers for pressure measurement.



Figure 8. Detail of a typical velocity profile. The rectangle on the right corresponds to the groove of the chamber for pressure measurement.

For a channel of height H , the fully developed profile of velocities is parallel to the membrane surface and has parabolic shape and depends on the average velocity U_t and is given by the Couette flow equation (3).

$$u_t(z) = 6U_t \cdot \left(\left(\frac{z}{H} \right) - \left(\frac{z}{H} \right)^2 \right) \quad (3)$$

This profile was compared with those obtained immediately after the groove of the pressure chamber for different positions of the pressure chamber (Figure 9). The profiles were obtained using the Line/Extrusion plot. It can be observed that it is necessary a distance of at 9 mm to have a velocity profile near to the laminar one on the membrane surface.

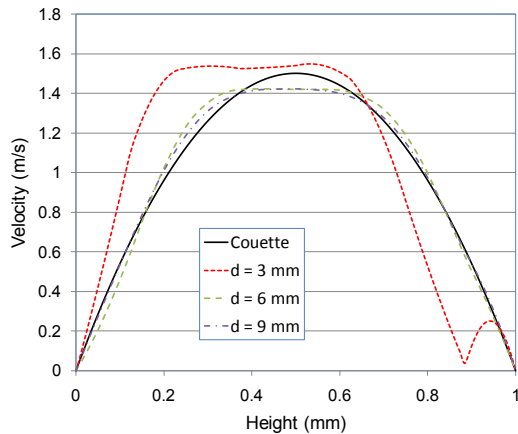


Figure 9. Velocity profiles in the separation between plates obtained with the 2D geometry.

The 3D geometry was used to obtain the pressure and velocity maps (Figures 10 and 11). It was confirmed that the pressure losses measured between the two pressures chambers could be very low (< 0.01 bar) compared to that

measured in other laboratory modules (0.1 – 0.5 bar).

It was also demonstrated that the flow profile became relatively homogeneous in most of the channel width, especially after the groove of the chamber for pressure measure (Figure 12). Using the values of the velocity profile, the shear rate on the membrane surface can be calculated. The result is important to explain differences in fouling experimentally observed on the membrane surface.

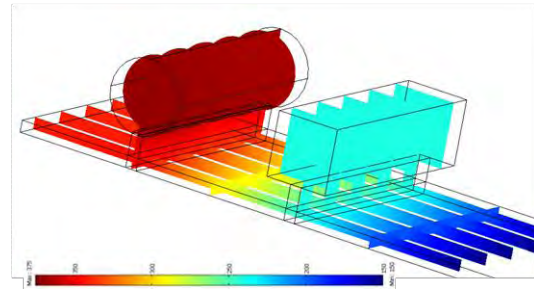


Figure 10. Pressure map

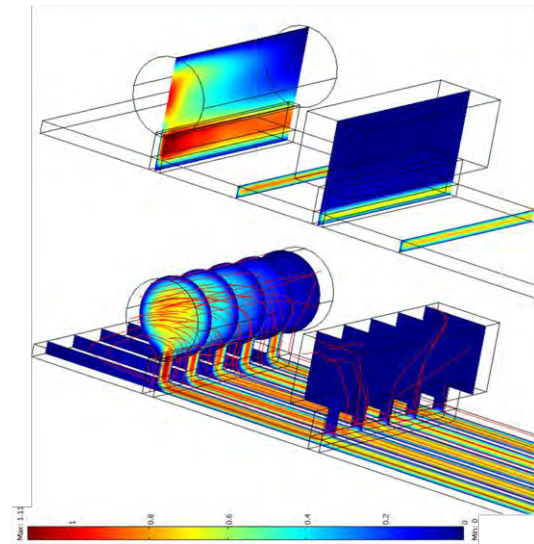


Figure 11. Velocity map and streamlines

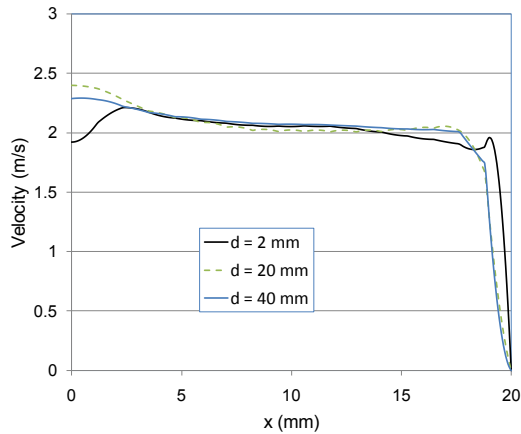


Figure 12. Velocity profiles along the width of the membrane channel for different distances to the entrance groove (height is half of the plate separation).

5. Mechanical analysis of the module

The analysis of the displacement for each plate at the chamber pressure revealed that it is not expected problems of excessive deformation at the limits of the membrane chamber where the seal is placed and consequently the system remains watertight (Figures 13 and 14).

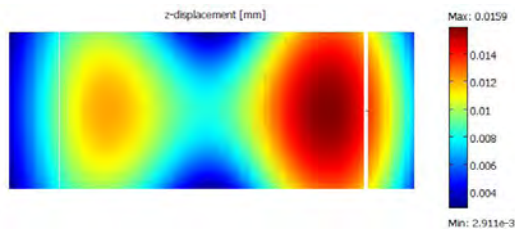


Figure 13. Displacement on the face of the membrane chamber of the upper plate at a pressure of 120 bar.

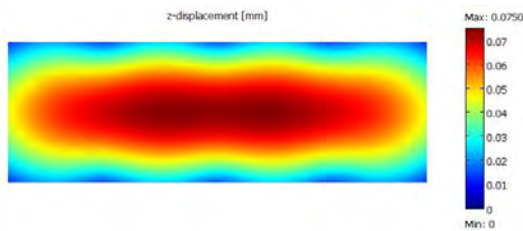


Figure 14. Displacement on the face of the membrane chamber of the lower plate at a pressure of 120 bar.

6. Conclusions

COMSOL Multiphysics was useful to evaluate the design of a flat module intended for laboratory research. The results allowed us to obtain the best position for two chambers for pressure measurement. The flow profiles obtained will be useful to understand differences on fouling on the membrane surface. Besides, the mechanical study of the module assured that the thickness selected for the module plates were suitable to resist the limiting pressures.

7. List of symbols

- d horizontal distance to groove, m
- H channel height, m
- p pressure, Pa
- \mathbf{u} velocity vector, m/s
- u_i velocity, m/s
- U_i average velocity in canal, m/s
- z height over membrane surface, m

- ρ density, $\text{kg}\cdot\text{m}^{-3}$
- η viscosity, $\text{Pa}\cdot\text{s}$

8. References

1. M. Mulder, *Basic principles of membrane technology (Transport in membranes)*, 210-278. Kluwer Academic Press, Netherlands (1996)
2. J.M. Gozávez-Zafrilla, A. Santafé-Moros, Aplicaciones del análisis mediante elementos finitos a la tecnología de membranas, *Proceedings of the Spanish COMSOL Conference*, Madrid, Spain (2008)
3. P. Henriksen, O. Hassager; Simulation of transport phenomena in ultrafiltration, *Chemical Engineering Science*, **48**, 2983-2999 (1993)
4. L. Huang and M.T. Morrissey; Finite element analysis as a tool for crossflow membrane filter simulation, *Journal of Membrane Science*, **155**, 19-30 (1999)
5. D.E. Wiley, D.F. Fletcher; Techniques for computational fluid dynamics modelling of flow in membrane channels, *Journal of Membrane Science*, **211**, 127-137 (2003)

6. S. Ma et al.; A 2-D streamline upwind Petrov/Galerkin finite element model for concentration polarization in spiral wound reverse osmosis modules, *Journal of Membrane Science*, **244**, 129-139 (2004)
7. A. Subramani, S. Kim, and E.M.V. Hoek; Pressure, flow, and concentration profiles in open and spacer-filled membrane channels, *Journal of Membrane Science*, **277**, 7-17 (2006)
8. S. Curcio et al., A theoretical analysis of transport phenomena in membrane concentration of liquorice solutions: a FEM approach *Journal of Food Engineering*, **71**, 252-264 (2005)
9. E. Lyster and Y. Cohen; Numerical study of concentration polarization in a rectangular reverse osmosis membrane channel: Permeate flux variation and hydrodynamic end effects, *Journal of Membrane Science*, **303**, 140-153 (2007)
10. R. Ghidossi, D. Veyret, and P. Moulin; Computational fluid dynamics applied to membranes: State of the art and opportunities, *Chemical Engineering and Processing*, **45**, 437-454 (2006)
11. D. Bhattacharyya et al.; Prediction of concentration polarization and flux behavior in reverse osmosis by numerical analysis, *Journal of Membrane Science*, **48**, 231-262 (1990)
12. W.R. Bowen, A.O. Sharif; Transport through microfiltration membranes - particle hydrodynamics and flux reduction, *J. Colloid Interface Sci.*, **168**, 414-421 (1994)
13. W.R. Bowen, H. Mukhtar; Characterisation and prediction of separation performance of nanofiltration membranes, *Journal of Membrane Science*, **112**, 263-274 (1996)
14. W.R. Bowen, A.O. Sharif; Hydrodynamic and colloidal interactions effects on the rejection of a particle larger than a pore in microfiltration and ultrafiltration membranes, *Chemical Engineering Science*, **53**, 879-890 (1998)
15. C.J. Richardson, V. Nassehi; Finite element modelling of concentration profiles in flow domains with curved porous boundaries, *Chemical Engineering Science*, **58**, 2491-2503 (2003)
16. O. Guseva, A.A. Gusev; Finite element assessment of the potential of platelet-filled polymers for membrane gas separations, *Journal of Membrane Science*, **325**, 125-129 (2008)
17. C. Siegel; Review of computational heat and mass transfer modeling in polymer-electrolyte-membrane (PEM) fuel cells, *Energy*, **33**, 1331-1352 (2008)
18. J. Sousa et al.; Modeling and simulation of the anode in direct ethanol fuels cells, *Journal of Power Sources*, **180**, 283-293 (2008)
19. A.E. Childress et al.; Mechanical analysis of hollow fiber membrane integrity in water reuse applications, *Desalination*, **180**, 5-14 (2005)
- Amy E. Childress, Pierre Le-Clech, Joanne L. Daugherty, Caifeng Chen, Greg L. Leslie
20. J.K. Guest, J.H. Prévost; Design of maximum permeability material structures, *Computer Methods in Applied Mechanics and Engineering*, **196**, 1006-1017 (2007)
21. D. Delaunay, M. Rabiller-Baudry, J.M. Gozávez-Zafrilla, B. Balannec et al.; Mapping of protein fouling by FTIR-ATR as experimental tool to study membrane fouling and fluid velocity profile in various geometries and validation by CFD simulation, *Chemical Engineering and Processing: Process Intensification*, **47**, 1106-1117 (2008)
22. J.M. Gozávez-Zafrilla, A. Santafé-Moros; Effect of backflushing on a particle inside a pore of a microfiltration membrane, *Proceedings of the COMSOL Users Conference in Grenoble*, **2**, 854-858 (2007)
23. J.M. Gozávez-Zafrilla, A. Santafé-Moros; Nanofiltration Modeling Based on the Extended Nernst-Planck Equation under Different Physical Modes, *Proceedings of the European COMSOL Conference*, Hannover, Germany (2008)
24. B. Balannec, J.M. Gozávez-Zafrilla, D. Delaunay, M. Rabiller-Baudry, Flow modeling in a flat membrane module, *Proceedings of the European COMSOL Conference*, Grenoble, France (2007)

9. Acknowledgements

The Universidad Politécnica de Valencia is kindly acknowledged for its financial support (PAID-06-08-3287)